

ITAPS front-tracking in energy research applications

Roman Samulyak^{1,2}, James Glimm^{1,2}, Xiaolin Li¹, Viktor Kilchyk^{1,2}, Paul Parks³, Tianshi Lu⁴, Wurigen Bo⁵

¹ Department of Applied Mathematics and Statistics, Stony Brook University, Stony Brook, NY 11794

² Computational Science Center, Brookhaven National Laboratory, Upton, NY 11973

³ General Atomics, P.O. Box 85608, San Diego, CA 92186-5608

⁴ Department of Mathematics and Statistics, Wichita State University, Wichita, KS 67260

⁵ Los Alamos National Laboratory, Los Alamos NM 87545

E-mail: rosamu@ams.sunysb.edu

Abstract.

New front-tracking technologies and the multiphysics code FronTier have been developed under the SciDAC project ITAPS. The front-tracking library is a software package for geometry and interface dynamics; the FronTier code includes hyperbolic, parabolic, and elliptic solvers for interface-bounded domains and physics models for compressible and incompressible fluid dynamics, magnetohydrodynamics, and phase transitions. Presented here are applications of FronTier to selected problems of the DOE program in energy research, namely, the simulation of pellet fueling of thermonuclear fusion devices, computational evaluation of new concept of magneto-inertial nuclear fusion, and design of high-power accelerator targets. Numerical simulations revealed new features of physics processes and provided computational support for the design and operation of experiments in high energy physics and fusion energy sciences.

1. Introduction

Multiphase flows play a significant role in numerous problems of fundamental and applied sciences and engineering. Accurate description of multiphase system components and their boundaries or interfaces is a challenging task for numerical simulations. Interfaces can be geometrically highly complex, and properties of single-phase components across interfaces can vary both qualitatively, requiring proper mathematical description, and quantitatively by orders of magnitude, imposing temporal and spatial scale restrictions.

Numerical study of multiphase systems has attracted considerable attention from researchers during past two decades, which has resulted in numerous methods and algorithms. An incomplete list include the level set method [1, 2], the volume-of-fluid method [3], the smoothed particle hydrodynamics method [4, 5], and the cubic-interpolated pseudo-particle method [6, 7]. The principal difference and advantage of the front tracking method for multiphase flows [8, 9] compared with the above-mentioned techniques is the explicit tracking of interfaces, which eliminates or greatly reduces the numerical diffusion and makes it easy to implement different physics laws for single components or the interface itself. The method of front tracking has laid the foundation for the multiphysics code FronTier [10]. Geometrical features of FronTier have been further developed within the SciDAC project Interoperable Technologies for Advanced

Petascale Simulations (ITAPS) [12]. A magnetohydrodynamic extension of the FronTier code has also been developed [13].

The method of front tracking and the FronTier code have been applied to numerous scientific and engineering problems (see [14] and references therein) ranging from fundamental studies of turbulent fluid mixing to accelerator and nuclear reactor design. In this paper, we describe the application of ITAPS front tracking to three problems of the Department of Energy research program in the area of nuclear fusion and high energy physics. In addition to detailed numerical studies of the corresponding physics processes, our simulations provided computational support for the design and operation of experiments in high energy physics and fusion energy sciences.

The paper is organized as follows. Section 2 describes the development of front-tracking technologies within the SciDAC ITAPS project. Applications of the front-tracking method to the problem of pellet fueling of thermonuclear fusion devices are described in Section 3. In Section 4, we apply the FronTier code to the simulation of plasma-jet induced magneto-inertial fusion. Numerical simulations of hydrodynamics and magnetohydrodynamic processes in high-power mercury targets are described in Section 5. We conclude the paper with a summary of our results and perspectives for the future work.

2. Numerical algorithms and their implementation

2.1. ITAPS front-tracking technologies

Front tracking is an adaptive computational method in which a lower-dimensional moving grid or interface (a triangulated surface in 3D space) represents a material interface [8, 9]. It is intrinsically a Lagrangian method in which a continuous geometrical manifold is represented and approximated by a discrete set of marker points defining the interface. Interface propagation is performed through solving an ODE along the local characteristics of each marker point. The method can give resolution at subgrid level and maintains sharp corners with acute angles. It is suitable for simulations with a rigid body boundary as well as with fluid interfaces that undergo complex rolling and deformation.

New algorithms have been recently introduced to make the front-tracking method more robust and efficient in topological bifurcation. Among them the most significant is the locally grid-based (LGB) method [12]. This method combines the accuracy of the generic grid-free tracking [9] and the robustness of the grid-based method in resolving the topological bifurcation, especially in three dimensions.

A set of standardized functions have been constructed to serve as a user interface for application programs. This includes the start-up functions, initialization for front geometry and velocity functions, query functions to access interface entities such as vertices, simplexes and manifolds, and functions for topological information. We have also built a set of functions for interpolation and interaction between a moving front and the supporting rectangular mesh.

The propagation of front points can be divided into two categories. The first is the propagation independent of interface geometry such as with a given velocity function of space and time or a velocity interpolated from the computational mesh. For this type of propagation, the order of accuracy in propagating the interface marker points can be made arbitrarily high as long as we use sufficiently high-order Runge-Kutta method along the local characteristics. In the second type of propagation, the front velocity depends on the geometry of the interface. A typical case is the velocity in normal direction to the interface that depends on curvature. For this type of propagation, any predictor calculation must be carried out for the entire manifold so that the velocity in the predictor state is based on the new geometry of the propagated manifold. Since calculation of curvature involves second order of derivatives along the interface, the CFL condition controlling the time step is parabolic. The LGB method is combined with this type of propagation to make the computation robust and accurate.

The front-tracking method has been combined with the adaptive mesh refinement (AMR).

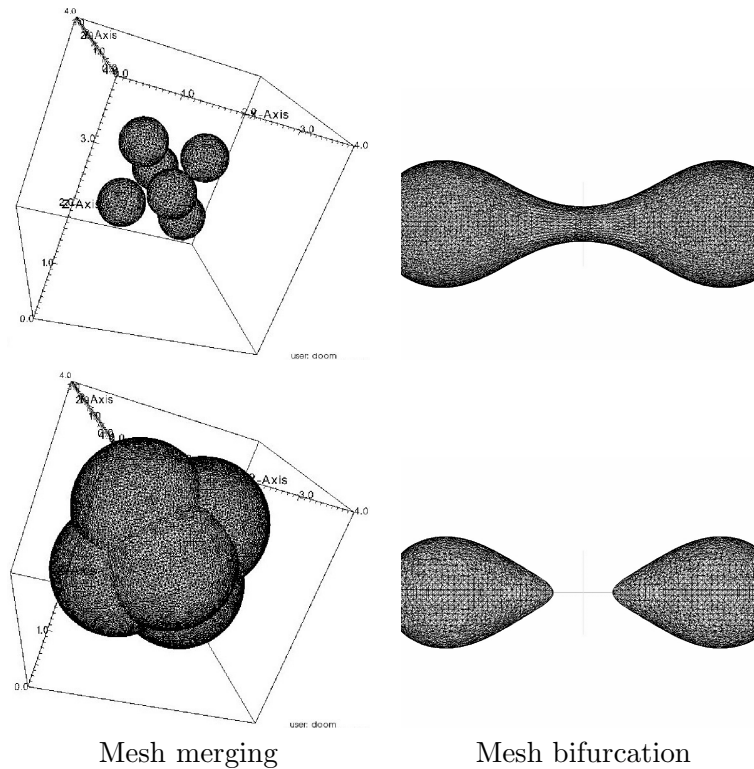


Figure 1. Three examples of the 3D FronTier code. From left: twisting, merging, and mesh bifurcation.

The coupling algorithm is based on cFluid, a modularized front-tracking code for compressible fluids, the geometrical FronTier-Lite library, and the SAMRAI AMR library. In this algorithm, the front propagation and ghost-fluid cell update are carried out only on the finest level of AMR patches, greatly reducing the need for the interlevel data communication of front geometry. This also allows the interface optimization and topological reconstruction to be performed on a uniform grid, that is, the finest level of the grid.

The front-tracking library is capable of propagating and robustly resolving topological changes of a large number of interfaces in two- and three-dimensional spaces. Figure 1 displays 3D tests for merging and bifurcation of surface meshes. Figure 2 demonstrates the geometric complexity of interfaces typical for FronTier simulations.

2.2. FronTier physics models

The front tracking-based FronTier code supports numerous physics models including multiphase compressible and incompressible fluid flows and magnetohydrodynamics in the low magnetic Reynolds number approximation [13]. Mathematically, these systems are described by coupled hyperbolic and parabolic or elliptic PDE's in geometrically complex and evolving domains bounded by interfaces. FronTier's hyperbolic methods include a TVD scheme and second-order MUSCL-type schemes with a collection of exact and approximate Riemann solvers. The elliptic equations are solved by using the embedded-boundary method [15] (see [16] for the latest development of the embedded-boundary method for 3D moving elliptic-interface problems with front tracking). High-performance, parallel software libraries of preconditioners and iterative solvers based on Krylov subspace methods such as PETSC are used for solving the corresponding linear system of equations.

FronTier's interface propagation algorithms of the predictor-corrector type depend on

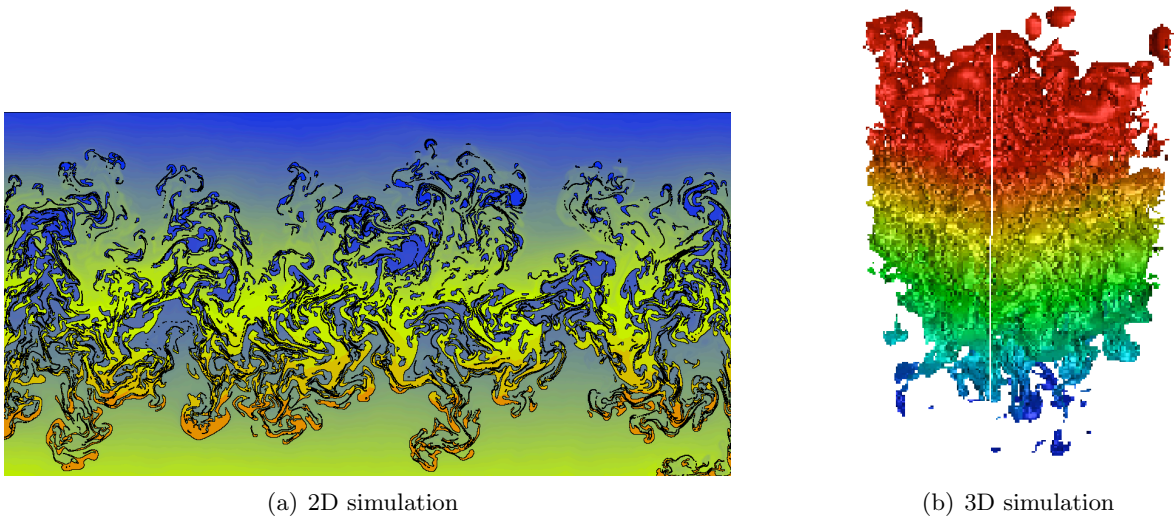


Figure 2. FronTier simulation of turbulent fluid mixing by Rayleigh-Taylor instability.

equations describing physics nature of components of the multiphase system. Examples include the propagation of phase boundaries during melting and solidification of incompressible phases [16] described by the Stefan problem. A novel phase boundary algorithm was developed in [17] to describe phase transitions in compressible fluids in which the interface mass flux is partially driven by nonlinear waves. An algorithm for propagation of interfaces in the presence of MHD components was developed in [13]. Subgrid-scale turbulence models have also been developed for the FronTier code. Various problem specific physics models will be mentioned in the context of applications in the next three sections.

3. Pellet ablation for ITER fueling

The International Thermonuclear Experimental Reactor (ITER) is a joint international research and development project that aims to demonstrate the scientific and technical feasibility of fusion power. In ITER, high-temperature plasma will be confined by magnetic fields in order to create and sustain conditions necessary for the fusion of deuterium and tritium atoms, and the corresponding energy release is expected to be bigger than energy required for the machine operation for the first time. In order to achieve this goal, ITER must be constantly fueled by the injection of small, frozen deuterium/tritium pellets [18]. To optimize the fueling process, the pellet ablation rate in the tokamak magnetic field must be accurately evaluated. This task requires numerical simulations with the resolution of complex physics processes occurring in the multiphase flow associated with the pellet ablation.

We first briefly summarize the main physics processes associated with the ablation of a cryogenic deuterium pellet in a tokamak magnetic field (see Fig. 3). Hot electrons traveling along the magnetic field lines hit the pellet surface, causing a rapid ablation. A cold, dense, and neutral gas cloud forms around the pellet and shields it from the incoming hot electrons. After the initial stage of ablation, the most important processes determining the ablation rate occur in the cloud. The cloud away from the pellet heats up above the dissociation and then the ionization levels, and partially ionized plasma channels along the magnetic field lines. As was shown in [19], this process can be described by the system of MHD equations in the low magnetic Reynolds number approximation. The plasma cloud stops the incident plasma ions at the cloud/plasma interface, while the faster incident electrons penetrate the cloud where their

flux is partially attenuated depending on the cloud opacity. We employ the kinetic model for the hot electron-plasma interaction proposed in [21]. The tendency of the background plasma to remain neutral confines the main potential drop to a thin sheath adjacent to both end-faces of the cloud. Inside the cloud, the potential slowly changes along each field line. Since the cloud density and opacity vary radially, the potential inside the cloud varies from field line to field line, causing $E \times B$ cloud rotation about the symmetry axis. The potential can be explicitly found by using kinetic models for hot currents inside the cloud [20]. The fast cloud rotation widens the ablation channel, redistributes the ablated gas, and changes the ablation rate.

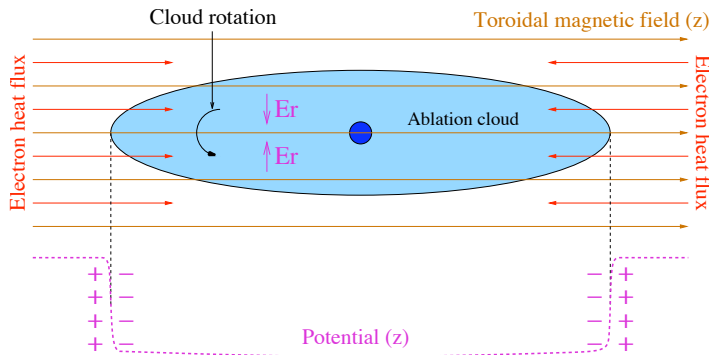


Figure 3. Schematic of physics processes associated with the ablation of deuterium pellet in a tokamak.

The numerical pellet ablation model was benchmarked in [19] using the theoretical neutral gas shielding model [22] and previous pure-hydrodynamic numerical simulations [21]. We reproduced the double transonic layer in the ablation cloud induced by atomic processes of dissociation and ionization (Fig. 4) and obtained an excellent agreement of cloud properties and ablation rates. Performing 2D pure hydrodynamic simulations, we explained the factor of 2.2 reduction of the pellet ablation rate of the axially symmetric model compared with the spherically symmetric one. In the literature, the effect was attributed to the directional heating [21]. We showed that the directional heating is responsible for only 18% of the ablation rate reduction, and the effect is caused mainly by the difference of ablation rates induced by the Maxwellian and monoenergetic electron heat fluxes [19].

Then we performed the first systematic studies of pellet ablation rates and channel properties in magnetic fields. The ionization of the pellet ablation cloud by the electron heat flux leads to the channeling of the ablation flow along magnetic field lines. We found that this effect is sensitive to the parameter “warm-up time” and the cloud rotation. Longer warm-up time leads to a slower increase of temperature and wider ablation flow channels. The rotation of the cloud widened the ablation channel. The channel radius increased from 2.3 cm without cloud rotation to 2.8 cm with rotation. The cloud pressure was lowered by 7%, and the pressure peak in the cloud was shifted to $r = 1.5$ cm. Along the z -axis, the density was lower with cloud rotation due to the centrifugal force, which corresponded to less shielding.

Figure 5 plots the Mach number of the rotational velocity $M_\theta = u_\theta/c$ for the steady-state flow with cloud rotation. It has transonic distribution, and the sonic points are located in the ablation channel and close to the channel boundary. With cloud rotation, the steady-state ablation rate increased from 195 g/s to 260 g/s. We conclude that the cloud rotation increases the ablation rate because of the widening of the ablation channel and redistribution of density in the channel. With the inclusion of the pellet cloud rotation model [23], simulated ablation rates agreed with experimental data on the pellet ablation.

4. Plasma jet induced magneto-inertial fusion

The main advantage of the magnetized target inertial fusion approach compared with the conventional inertial confinement fusion, which has no embedded magnetic field, is the potential

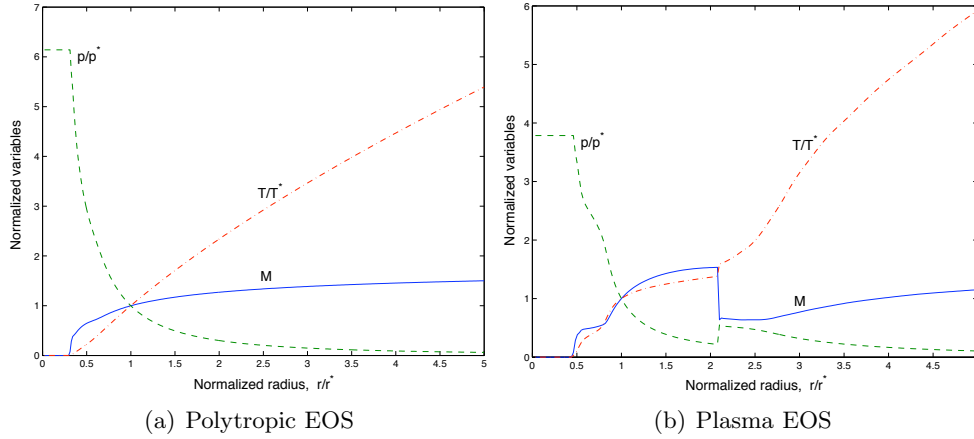


Figure 4. Normalized ablated gas profiles at $10\ \mu\text{s}$ in 1D spherically symmetric model of (a) ablation without atomic processes (polytropic EOS), and (b) with atomic processes (plasma EOS). The solid, dashed, and dash-dotted lines are M , p/p^* , and T/T^* as functions of r/r^* , respectively.

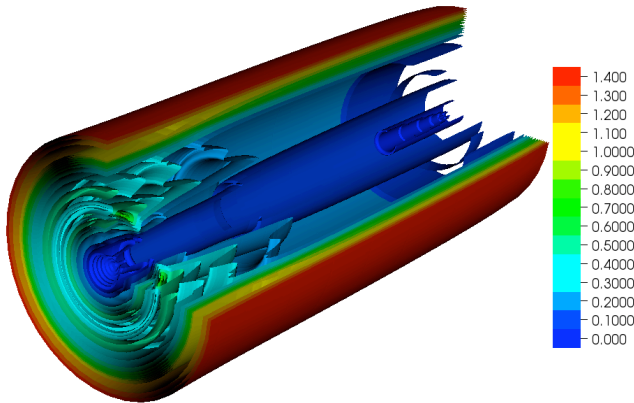


Figure 5. Isosurfaces of Mach number in the steady-state ablation cloud.

for reducing the driver power needed to achieve ignition conditions in the central hot spot [24, 25]. In the magnetized target, the transport of heat and energetic fusion alpha particles is greatly reduced. The conventional magneto-inertial fusion method uses an imploding solid metal liner in cylindrical or spherical geometry to adiabatically compress a preformed magnetized plasma target [26]. The proposed targets are either spherical ones formed by two compact toroids of fusion materials containing magnetic fields or linear targets, such as a Z-pinch [27].

A longstanding concern with most solid liner driven MIF concepts is the “stand-off problem”: the target-related hardware has to be located at a sufficient stand-off distance from the fusion hot spot in order to be reusable. Another important concern is the solid liner manufacturing cost. To solve these problems, Thio *et al.* [28] suggested that a spherical array of supersonic plasma jets launched from the periphery of the implosion chamber could be used to create a spherically symmetric plasma liner to implode the central magnetized target. Such a plasma liner is assembled when the jets intersect and merge with each other at an intermediate radius r_m , as shown schematically in Figure (6). The purpose of our work is to evaluate the concept of plasma-jet induced magneto-inertial fusion (PJMIF) via numerical simulations and to provide computational support for the Plasma Liner Experiment being built at Los Alamos National Laboratory.

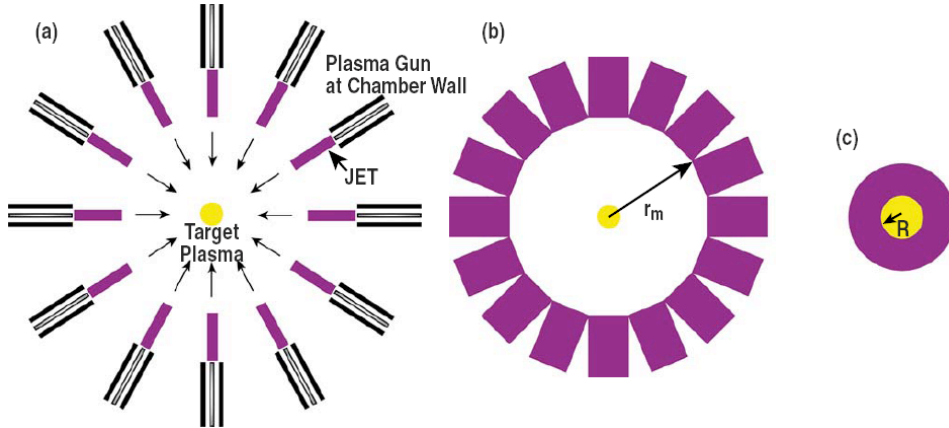


Figure 6. Schematic of the plasma jet induced magnetized target fusion. (a) Plasma guns at the chamber wall shoot high velocity, supersonic plasma jets. (b) Jets merge at the merging radius r_m and form a liner. (c) Plasma liner implodes and compresses the target.

4.1. Spherically symmetric simulations

To obtain first-order estimates of conditions achievable in PJMIF and the corresponding fusion energy gain and to compare numerical simulations with theoretical predictions, we performed spherically symmetric simulations of the implosion of plasma liners and compression of plasma targets [31]. The cases of single deuterium and xenon liners and double-layer deuterium-xenon liners compressing various deuterium-tritium targets have been investigated, optimized for maximum fusion energy gains, and compared with theoretical predictions and scaling laws of [30]. In agreement with the theory, the fusion gain was significantly below unity for deuterium-tritium targets compressed by Mach 60 deuterium liners. In the most optimal setup for a given chamber size that contained a target with the initial radius of 20 cm compressed by 10 cm thick Mach 60 xenon liner, the target ignition and fusion energy gain of 10 was achieved. We also investigated the effect of self-heating of plasma targets by alpha particles. Naturally, the importance of this effect depends on the presence of fusion events in the target. Negligible for the case of deuterium liners, the alpha-particle heating became significant for xenon liners: it increased the fusion gain of 20 cm liner from 6 to 10.

4.2. Equation of state with atomic physics processes

To account for atomic physics processes in plasma liners, we have developed new EOS models for FronTier. The processes of dissociation (in diatomic gases like deuterium) and ionization introduce energy sinks and therefore strongly affect the plasma temperature. The complete deuterium EOS with atomic processes was developed by us in [19] and used for the simulation of the pellet ablation in tokamaks and the implosion of deuterium plasma liners. The presence of atomic physics processes lowers the liner temperature, increases the Mach number of the liner (by 40% at the late stages of the implosion), increases the stagnation pressure in the target by more than 30%, and increases the fusion energy gain.

The equation of state for high-Z materials such as argon or xenon, which have multiple ionization levels, requires the solution of coupled system of Saha equations [32]. An iterative solution for such a large system of coupled nonlinear equations is possible as a stand-alone calculation but is prohibitively expensive in a hydrodynamic code if performed in each point at each time step. We have overcome this problem by using ideas of an average ionization model proposed by Zeldovich [32]. By introducing a notion of average ionization, the coupled system of Saha equations can be reduced to a differential equation, and the problem computationally

reduces to finding a root of one complex nonlinear equation. Efficient solvers implementing this method have been developed for the FronTier code.

4.3. 3D liner implosion

In this section, we summarize results of 3D simulations of the formation and implosion of plasma liners. The simulation consists of three stages. In the first stage, we performed axially symmetric simulations of the propagation of detached plasma jets from the plasma gun nozzle to the merging radius. The purpose of the detached jet simulation is to obtain profiles of density, pressure, and velocity in jets before their merger and to provide input for 3D simulations of the liner formation.

Using the results of the detached jet simulation, we initialized 3D jet merger simulations by (1) finding directions of N jets uniformly distributed in space and (2) initializing states around each direction using pressure, density, and velocity profiles from the detached jet simulation. The problem (1), equivalent to the uniform distribution of N points on a unit sphere, is solved by using spherical centroidal Voronoi tesslation (SCVT). We solve the SCVT problem iteratively as a constrained minimization problem. The initialization of states was obtained by performing 3D Cartesian to 2D cylindrical coordinate transformations and using the corresponding numerical data sets with bilinear interpolation.

We have examined the merger of 144 jets in a 6-meter radius chamber as well as 125 and 625 jets in a 3-meter radius chamber. We have investigated the heating of the liner by oblique shock waves and the corresponding reduction of the Mach number, and the liner uniformity with the change of the merging radius and increase of the number of jets. At the late stages of implosion, the Mach number of the 3D liners was several times lower of that of the corresponding 1D liners that resulted in the reduction of stagnation pressure by two orders of magnitude. We have concluded that oblique shock waves, generated during the liner formation, significantly reduce abilities of plasma liners to compress targets. We have also observed a strong influence of nonideal vacuum in the chamber on the self-implosion of liners. Pressure profiles in three-dimensional liner implosion simulations at 5, 10, and 50 microseconds are shown in Figure 7. Studies of the Rayleigh-Taylor instabilities in plasma targets will be the focus of our future research.

5. High-power liquid mercury targets

In this section, we apply the front-tracking algorithms for multiphase MHD to the simulation of the mercury target for the proposed Neutrino Factory/Muon Collider (<http://www.cap.bnl.gov/mumu/>). The purpose of the target is to convert powerful beams of protons into pions with the lifetime of 26 ns that decay into long-lived muons and neutrinos. The target will contain a series of 30-cm-long and mercury jets 1 cm in diameter entering a strong (~ 15 Tesla) magnetic field at a small angle to the solenoid axis (Figure 8). When each jet reaches the center of the solenoid, it interacts with a powerful proton pulse penetrating the jet and depositing energy of the order of 100 J/g into mercury. The purpose of our numerical simulations is to evaluate states of the target before and after the interaction with protons, in order to optimize the target design and to provide computational support for the MERIT targetry experiment that took place at the CERN proton driver in the fall of 2007. This section summarizes results of [34].

5.1. Simulation of the mercury jet entering a solenoid magnet

The nonuniform transverse component of the magnetic field with respect to the jet trajectory, caused by a small angle between the jet and the magnetic solenoid axis, distorts the jet during the motion toward the solenoid center. To evaluate the state of the jet target before the interaction with the solenoid axis, we performed numerical simulations of the jet entering the solenoid using the real profile of the magnetic field along the jet trajectory in the MERIT experiment.

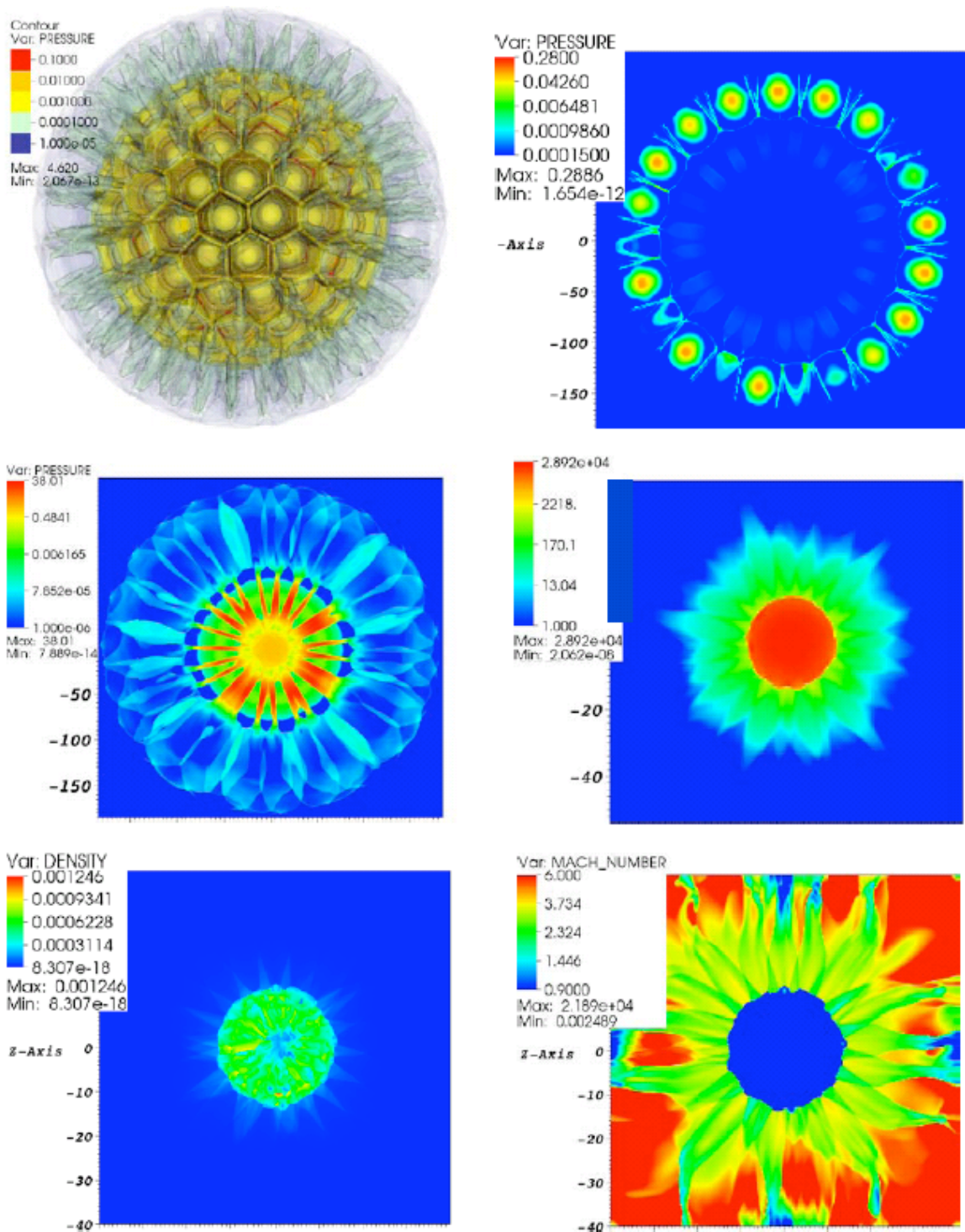


Figure 7. Pressure profiles in three-dimensional liner implosion simulations at 5, 10, and 50 microseconds.

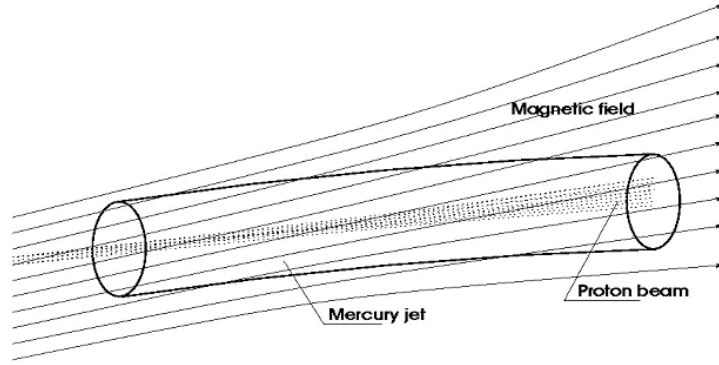


Figure 8. Schematic of the mercury jet target for Neutrino Factory/Muon Collider.

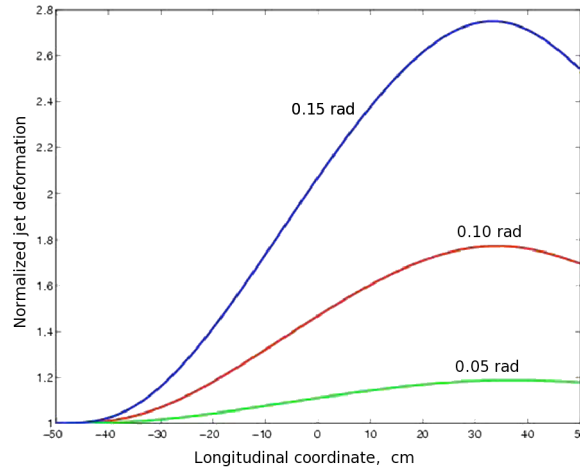


Figure 9. Normalized elliptic deformation of the mercury jet entering a 15 T solenoid at the angle of 0.15 rad (top line), 0.1 rad (middle line), and 0.05 rad (bottom line) to the magnetic axis.

Results are summarized in Figure 9, which plots the transverse-distortion ratio of the jet or the maximum radius in the transverse cross section normalized by the unperturbed initial radius of the jet. We observe that the distortion strongly depends on the angle between the jet and the solenoid axis: the maximum distortion ranges from 1.2 at the angle of 0.05 rad to 2.75 at the angle of 0.15 rad. The latter distortion is unacceptable for the target: it transforms the jet into a thin sheet and significantly reduces the effective cross section with the proton pulse and, as a result, the pion-production rate. In order to reduce the amount of distortion, the angle of 0.033 rad was used in the MERIT experiment.

5.2. Simulation of the mercury jet interacting with proton pulses

When the mercury jet reaches the solenoid center, it interacts with a proton pulse, depositing energy of the order of 100 J/g into mercury. Because of the short time scale of the interaction, we assume that the increase of the internal energy and pressure is isochoric. In computations, we modify the internal energy and pressure states of the jet during the initial time step according to predictions of atomistic Monte-Carlo simulations of the mercury - proton pulse interaction using the MARS code [35]. Because the shape of the jet is distorted by the transverse component of the magnetic field as described in the previous section, the cross section of the jet before

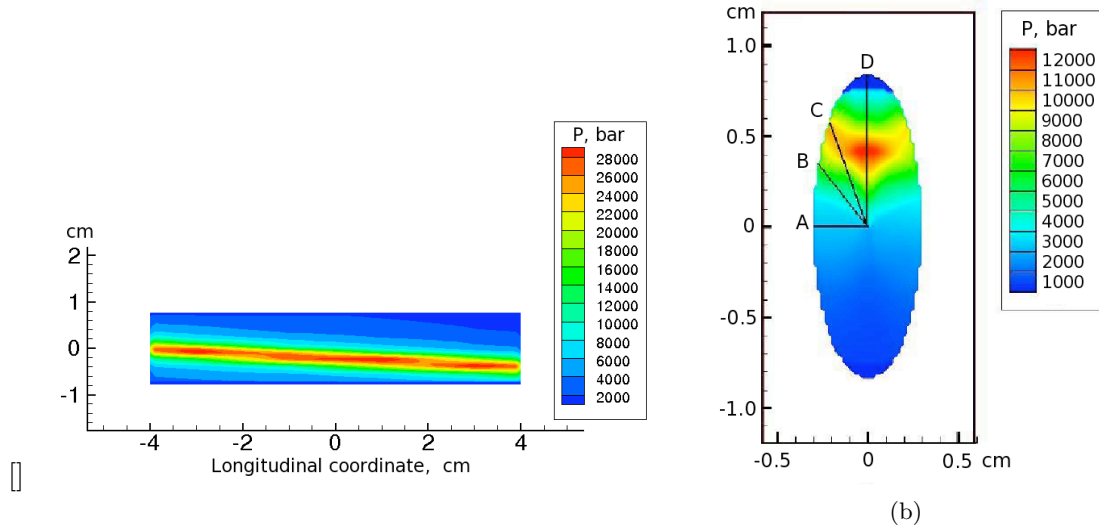


Figure 10. Pressure distribution in mercury after the interaction with proton pulses. Left image: cylindrical jet with a 24 GeV, 10-teraproton pulse. Right image: elliptic jet with a 14 GeV, 10-teraproton pulse.

the interaction with protons is an ellipse, with the long and short radii of 0.8 and 0.4 cm, correspondingly. The profiles of pressure after the interaction with 24 GeV, 10-teraproton and 14 GeV, 10-teraproton pulses are shown in Figure 10. For the mercury jet with the elliptic cross section, we monitored the jet surface velocity in four radial directions, or points A, B, C, and D shown in Figure 10(b).

After the energy deposition, the high-pressure wave propagates outward and reflects from the mercury-air interface as a strong rarefaction wave. With a single-phase equation of state model for mercury, the level of tension in the position of rarefaction wave crossings can reach dozens of kilobars. Since the mercury is unable to sustain such a strong tension, cavitation bubbles form that change properties of mercury and the dynamics of the jet response. Jet cavitation and the growth of cavitation bubbles cause a reduction of tension, rapid jet expansion, and surface instabilities. To model these processes in the mercury jet, we have developed a discrete bubble cavitation model for FronTier, in which tracked-surface cavitation bubbles are dynamically inserted with certain density in rarefaction waves that exceed a critical tension that depends on details of the problem (purity of the fluid, time scales, uniformity of tension etc.). A snapshot of cavitation bubbles in the jet is shown in Figure 11.

If the jet cavitation and expansion occur in a longitudinal magnetic field, the radial motion of the fluid induces vortices of azimuthal current, and the Lorentz force tends to suppress the fluid motion across the magnetic field lines. Hence the magnetic field reduces the amount of cavitation and partially stabilizes the mercury jet. Snapshots of the jet surfaces at 100 μ s after the interaction with the proton pulse in magnetic fields ranging from 0 to 15 Tesla are shown in Figure 12.

Figures 13–14 show the evolution of velocities of elliptic-jet surface filaments in four radial directions A, B, C, and D, as explained above. The maximum velocity of filaments ejected in the direction of the short axis reaches 35 m/s. In all directions, the velocity decreases with the increase of the magnetic field strength. We emphasize that the formation and evolution of filaments cannot be attributed solely to classical fluid interface instabilities such as the Rayleigh-Taylor and Richtmyer-Meshkov instabilities. We have shown that the formation of mercury jet filaments critically depends on the presence of cavitation. Simulated values of the velocity of

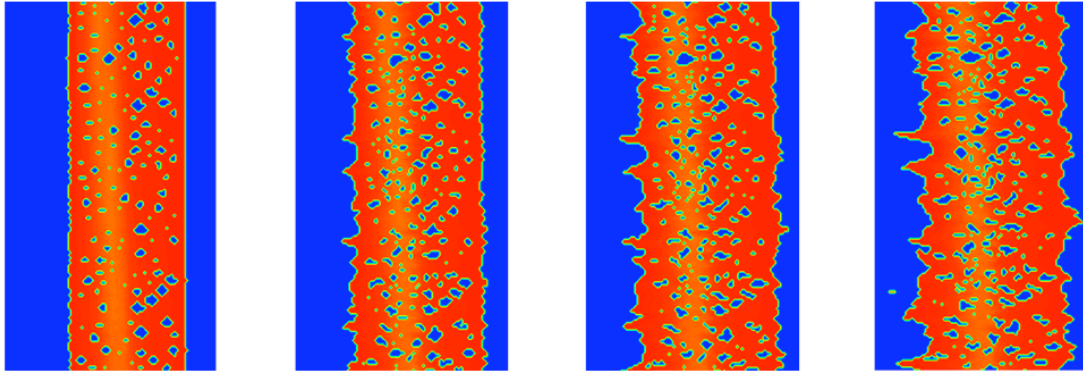


Figure 11. Cavitation bubbles in the mercury jet at 20, 130, 200, and 250 μs after the interaction of the cylindrical jet with the proton pulse.

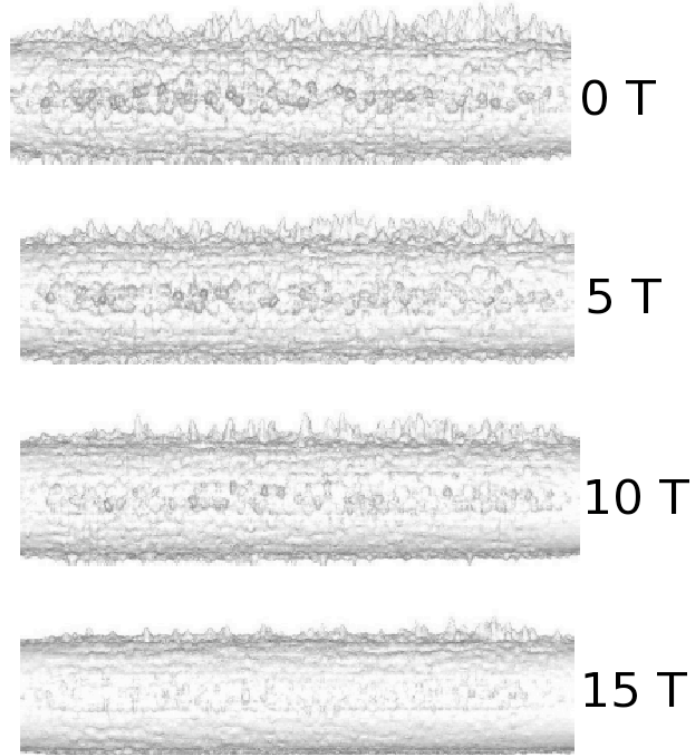


Figure 12. Filaments on the surface of initially cylindrical jet at 150 μs after the interaction with the proton pulse in magnetic fields ranging from 0 to 15 Tesla.

spikes were in good agreement with the MERIT experimental data at several values of the applied longitudinal magnetic field.

6. Conclusions and future plans

New front-tracking technologies and the FronTier code have been developed under the SciDAC project ITAPS. The front-tracking library is a software package for geometry and interface

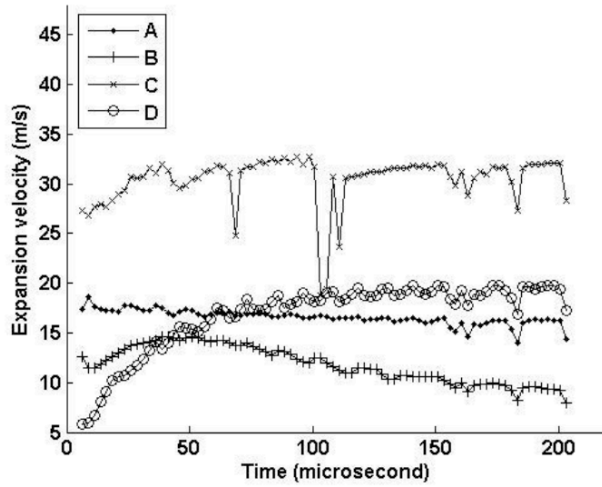


Figure 13. Expansion velocity of jet surface filaments without magnetic field.

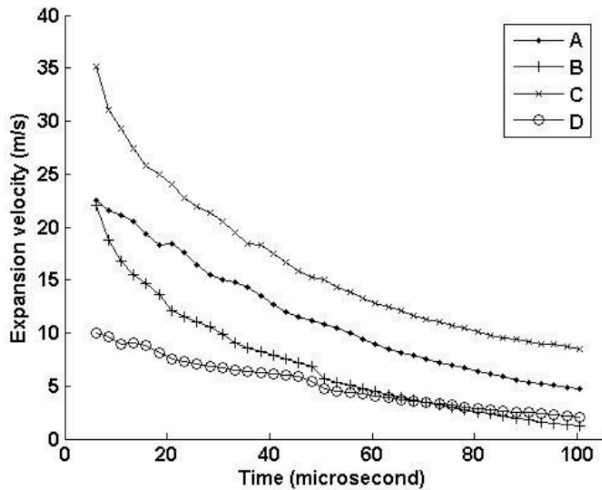


Figure 14. Expansion velocity of jet surface filaments in 15 Tesla magnetic field.

dynamics; FronTier is a multiphysics software framework based on front tracking for the simulation of systems of conservation laws. It includes hyperbolic, parabolic, and elliptic solvers for interface-bounded domains and physics models for compressible and incompressible fluid dynamics, magnetohydrodynamics, and phase transitions. The paper presents applications of FronTier to selected problems of the DOE energy research program, such as the pellet fueling of thermonuclear fusion devices, the new concept of magneto-inertial nuclear fusion based on supersonic plasma jets, and high-power accelerator targets. Numerical simulations revealed new features of physics processes and provided computational support for the design and operation of experiments in high energy physics and fusion energy sciences.

In our work on the pellet ablation, the ablation rate and lifetime in magnetic fields were systematically studied for the first time and compared with theory and existing experimental databases. Simulations revealed several new features of the pellet ablation. In the MHD

simulations, the Lorentz force funnels the ablation flow into an extended plasma shield, which intercepts the incident plasma heat flux and reduces the ablation rate, depending on the rise time of the heat flux seen by the pellet. Shorter warm-up times lead to narrower ablation channels and reduced ablation rate. This new feature implied that pellets transversing strong plasma gradients, as in the edge pedestal region of the ITER plasma, could have significantly lower ablation rates (higher fueling efficiency) if injected at higher velocity. Using a new model for the potential distribution in the ablation channel, we also demonstrated the supersonic rotation of the channel, a phenomenon most likely causing the striation instabilities.

ITAPS front-tracking technologies have been used in computational studies of the plasma jet-driven magneto-inertial fusion. The goal of simulations was to evaluate the method by estimating the fusion energy gain and to provide computational support for the plasma liner experiment being built at Los Alamos. In the first phase of research, we optimized the nuclear fusion gain in the liner target parameter space via spherically symmetric simulations. Single- and double-layer deuterium and xenon liners have been investigated as well as liners to be used in the PLX experiment. By varying target and liner parameters, the implosion process was optimized for maximum fusion energy gain and compared with theoretical predictions and scaling laws. In the most optimal setup, fusion ignition and energy gain of 10 was achieved with energy release of 10 GJ. We have performed 3D simulations of the merger of 144 jets in a 6-meter radius chamber as well as 125 and 625 jets in a 3-meter radius chamber. We have investigated the heating of the liner by oblique shock waves and the corresponding reduction of the Mach number, and the liner uniformity with the change of the merging radius and increase of the number of jets. We have concluded that oblique shock waves, generated during the liner formation, significantly reduce abilities of plasma liners to compress targets. In the future, we will study processes in the plasma target.

We have performed mathematical modeling, software development, and simulations of liquid mercury jet targets interacting with high-power proton beams in magnetic fields for the Neutrino Factory/Muon Collider Collaboration. Simulations aimed to make predictions for the first large targetry experiment at CERN called MERIT. MHD simulations predicted strong distortion of the jet entering the 15-Tesla solenoid and the reduction of the target efficiency. These studies have led to the change of design parameters of the MERIT experiment. Simulation also predicted strong instabilities and cavitation of the mercury jet interacting with proton pulses at zero magnetic field, as well as strong stabilizing effects of the magnetic field. Simulation predictions were confirmed by the MERIT experiment conducted at CERN. After the MERIT experiment, simulation work focuses on the full benchmark with experimental data and evaluation of the target behavior in the proton beam parameter range relevant to designs of the Muon Collider and Neutrino Factory.

Acknowledgments

This research utilized resources at the New York Center for Computational Sciences at Stony Brook University/Brookhaven National Laboratory which is supported by the U.S. Department of Energy under Contract No. DE-AC02-98CH10886 and by the State of New York.

References

- [1] S. J. Osher, R. P. Fedkiw, *Level Set Methods and Dynamic Implicit Surfaces*, Springer-Verlag 2002.
- [2] J. Sethian, *Level Set Methods and Fast Marching Methods: Evolving Interfaces in Computational Geometry, Fluid Mechanics, Computer Vision, and Materials Science*. Cambridge University Press, 1999.
- [3] C. W. Hirt, B. D. Nichols, Volume of fluid (VOF) method for the dynamics of free boundaries, *J. Comput. Phys.*, 39 (1981), 201225.
- [4] J.J. Monaghan, An introduction to SPH, *Computer Physics Communications*, 48 (1988), 8896.
- [5] Monaghan, J.J., Smoothed Particle Hydrodynamics, *Ann. Rev. Astron. Astrophys.*, 30 (1992), 543-74.

- [6] H. Takewaki, A. Nishiguchi and T. Yabe, The cubic-interpolated pseudo-particle(CIP) method for solving hyperbolic-type equations, *J. Comput. Phys.*, 61 (1985), 261-268.
- [7] T. Yabe et al., A universal solver for hyperbolic equations by cubic-polynomial interpolation, I and II (two and three-dimensional solvers), *Comput. Phys. Commun.*, 66 (1991) 219-242.
- [8] I. R. Chern, J. Glimm, O. McBryan, B. Plohr, S. Yaniv, Front tracking for gas dynamics, *J. Comput. Phys.*, 62 (1986) 83-110.
- [9] J. Glimm, J. Grove, X. L. Li, K. L. Shyue, Q. Zhang., Y. Zeng, Three dimensional front tracking, *SIAM J. Sci. Comput.*, 19 (1998) 703-727.
- [10] J. Glimm, J. Grove, X. L. Li, D. C. Tan, Robust computational algorithms for dynamic interface tracking in three dimensions, *SIAM J. Sci. Comput.*, 21 (2000) 2240-2256.
- [11] B. Fix, J. Glimm, X. Li, Y. Li, X. Liu, R. Samulyak, Z. Xu, A TSTT integrated FronTier code and its applications in computational fluid physics, *Journal of Physics: Conf. Series*, 16 (2005), 471 - 475.
- [12] J. Du, B. Fix, J. Glimm, X. Jia, X. Li, Y. Li, L. Wu. A simple package for front tracking, *J. Comput. Phys.*, 213 (2006), 613-628.
- [13] R. Samulyak, J. Du, J. Glimm, Z. Xu, A numerical algorithm for MHD of free surface flows at low magnetic Reynolds numbers, *J. Comp. Phys.*, 226 (2007), 1532 - 1549.
- [14] W. Bo, B. Fix, J. Glimm, X. Li, X. Liu, R. Samulyak, L. Wu FronTier and Applications to Scientific and Engineering Problems, *Proc. in Appl. Math. and Mech.*, 7 (2007), 1024507.
- [15] H. Johansen, P. Colella, A Cartesian grid embedded boundary method for Poisson's equation on irregular domains, *J. Comput. Phys.*, 147 (1998) 60-85.
- [16] S. Wang, R. Samulyak, T. Guo, An embedded boundary method for parabolic problems with interfaces and application to multi-material systems with phase transitions, *Acta Mathematica Scientia*, 30B (2010), No. 2, 499-521.
- [17] Z. L. Xu, T. Lu, R. Samulyak, J. Glimm, X. M. Ji, Dynamic phase boundaries for compressible fluids, *SIAM J. Sci. Computing*, 30 (2008), No. 2, 895-915.
- [18] Pegourie B Review: Pellet injection experiments and modelling, *Plasma Phys. Control. Fusion*, 49 (2007) R87-R160.
- [19] R. Samulyak, T. Lu, P. Parks, A magnetohydrodynamic simulation of pellet ablation in the electrostatic approximation, *Nuclear Fusion*, 47 (2007) 103-118.
- [20] P. Parks, Theory of pellet cloud oscillation striations, *Plasma. Phys. Control. Fusion*, 38 (1996) 571-591.
- [21] R. Ishizaki, P. Parks, N. Nakajima, M. Okamoto, Two-dimensional simulation of pellet ablation with atomic processes, *Phys. Plasmas*, 11 (2004), 4064-4080.
- [22] P. Parks, R. Turnbull, Effect of transonic flow in the ablation cloud on the lifetime of a solid hydrogen pellet in plasma, *Phys. Fluids*, 21 (1978), 1735-1741.
- [23] P. Parks, T. Lu, R. Samulyak, Charging and $E \times B$ rotation of ablation clouds surrounding refueling pellets in hot fusion plasmas, *Physics of Plasmas*, 16, 060705 (2009).
- [24] R. C. Kirkpatrick, I. R. Lindemuth, and M. S. Ward, *Fusion Technol*, 1995, Vol. 27, p. 201.
- [25] A. Hasegawa, K. Nishihara, H. Daido, M. Fujita, R. Ishizaki, F. F. Miki, K. Mima, M. Murakami, S. Nakai, K. Terai, and C. Yamanaka, *Nucl. Fusion*, 1988, Vol. 28, p. 369.
- [26] A. Sherwood, *Megagauss Physics and Technology. Second International Conference on Megagauss Magnetic Field Generation and Related Topics*, Washington, D.C. (Plenum, New York, 1980), p. 375.
- [27] D.D. Ryutov, M.S. Derzon, and M.K. Matzen, The physics of fast Z-pinchs, *Rev. Mod. Phys.*, 2000, Vol. 72, p. 167.
- [28] Y. C. F. Thio, E. Panarella, R. C. Kirkpatrick, C. E. Knupp, F. Wysocki, P. Parks, G. Schmidt, Magnetized target fusion in a spheroidal geometry with standoff drivers, in *Current Trends in International Fusion Research II*, edited by E. Panarella, National Research Council Canada, Ottawa, Canada, 1999.
- [29] Y. C. Francis Thio and Ronald. C. Kirkpatrick. Magnetized target fusion driven by plasma liners. In *Annual Meeting of the American Nuclear Society*, Hollywood, FL, 2002.
- [30] P. Parks, On the efficacy of imploding plasma liners for magnetized fusion target compression, *Phys. Plasmas* 15, 062506 (2008).
- [31] R. Samulyak, P. Parks, L. Wu, Spherically symmetric study of plasma liner implosion for magnetized target fusion, *Physics of Plasmas*, 17 (2010), 092702.
- [32] Ya. B. Zel'dovich, Yu. P. Raizer, *Physics of shock waves and high-temperature hydrodynamic phenomena*, Dover Publications, 2002.
- [33] R. Samulyak, H. Kim, L. Zhang, P. Parks, The influence of ionization on implosion of plasma liners, submitted to *Physics of Plasmas*, 2011.
- [34] R. Samulyak, W. Bo, X. Li, H. Kirk, K. McDonald, Computational algorithms for multiphase magnetohydrodynamics and applications, *Condensed Matter Physics*, 13 (2010), No. 4, 43402: 1-12.
- [35] S. Striganov, MARS15 simulations of the MERIT Mercury Target Experiment, *Third High-Power Targetry*

Workshop, Bad Zurzach, Switzerland, September 13, 2007.